



Cite this: *J. Mater. Chem. B*, 2023, 11, 8464

## A general method for endowing hydrophobic nanoparticles with water dispersion abilities†

Han Wang,<sup>a</sup> Zi Fu,<sup>a</sup> Xiuru Ji,<sup>a</sup> Min Lu,<sup>a</sup> Lianfu Deng,<sup>a</sup> Zhuang Liu,<sup>\*b</sup> Bo Yin<sup>\*c</sup> and Dalong Ni<sup>†\*</sup>

Inorganic nanoparticles with long-chain ligands are usually hydrophobic. However, simple and practical methods for converting hydrophobic nanoparticles to hydrophilic nanoparticles are still lacking. Herein, we developed a general method involving using dimercaptosuccinic acid (DMSA) for endowing hydrophobic nanoparticles with water dispersion abilities. By mixing a tetrahydrofuran solution of DMSA with a cyclohexane solution of hydrophobic nanoparticles, the long-chain ligands were replaced with DMSA, with the replacement due to the strong and broad-spectrum coordination abilities of sulphhydryls and carboxyls. Four representative kinds of hydrophobic nanoparticles, namely Ag, NaGdF<sub>4</sub>, TiO<sub>2</sub>, and ZnS nanoparticles, were selected for verifying the performance of this DMSA-based modification method. Meanwhile, this method can also widen the applications of hydrophobic nanoparticles and facilitate their being subjected to further graft modifications. We hope that our research will increase the chances for applications of nanomaterials to be made.

Received 16th May 2022,  
Accepted 7th August 2023

DOI: 10.1039/d2tb01038k

rsc.li/materials-b

### Introduction

Pyrolysis methods are widely used for the synthesis of inorganic nanomaterials, and could produce monodispersed, uniform and well-crystallized nanomaterials more easily than other methods. Pyrolysis has been used to synthesize many kinds of nanomaterials including rare earth (Re) materials (NaReF<sub>4</sub>, Re<sub>2</sub>O<sub>3</sub>, etc.), magnetic nanoparticles (Fe<sub>3</sub>O<sub>4</sub>, etc.), metal nanoparticles (Pd, Fe, Ag, etc.) and metal chalcogenides (ZnS, FeS<sub>2</sub>, Cu<sub>2-x</sub>Se, etc.).<sup>1–10</sup> Generally, long-chain ligands including oleic acid (OA), oleylamine (OAm), and octadecylamine (OctAm) need to be included when carrying out pyrolysis synthesis, because these ligands can act as reaction solvents, assist to form the precursor, and control the growth of a certain crystal face.<sup>10–12</sup> However, the generated nanomaterials with long-chain ligands are hydrophobic, with this feature not suitable for biological applications.

In the past decade, various methods have been developed to endow hydrophobic nanoparticles with water dispersion abilities for broader applications in medicine.<sup>13–20</sup> Generally, to show water dispersion abilities, the long-chain ligands should be replaced with water-soluble ligands. For example, nitrosonium tetrafluoroborate (NOBF<sub>4</sub>) has been reported to replace OA and OAm ligands reversibly.<sup>14</sup> Polyethylene glycol (PEG)-derivatized phosphine oxide (PO-PEG) has been reported to replace the OA ligands of metal oxide nanoparticles, while the Lemieux-von Rudloff reagent (*i.e.*, KMnO<sub>4</sub> and NaIO<sub>4</sub>) was used for oxidizing the carbon-carbon double bond of OA to obtain azelaic acid ligands.<sup>15,16</sup> However, some issues remain with

<sup>a</sup> Department of Orthopaedics, Shanghai Key Laboratory for Prevention and Treatment of Bone and Joint Diseases, Shanghai Institute of Traumatology and Orthopaedics, Ruijin Hospital, Shanghai Jiao Tong University School of Medicine, Shanghai 200025, China. E-mail: ndl12353@rjh.com.cn

<sup>b</sup> Department of Radiology, Fudan University Shanghai Cancer Center, Shanghai 200032, China. E-mail: liuzhuang201010@126.com

<sup>c</sup> Department of Radiology, Huashan Hospital, Fudan University, Shanghai 200040, China. E-mail: yinbo@fudan.edu.cn

† Electronic supplementary information (ESI) available: Experimental details and supplementary data. See DOI: <https://doi.org/10.1039/d2tb01038k>



Dalong Ni

Dalong Ni received his PhD degree in 2016 from the Shanghai Institute of Ceramics, Chinese Academy of Sciences (SICCAS), followed by a postdoctoral training in the Department of Radiology at the University of Wisconsin-Madison. At present, he is a Full Professor at the Shanghai Jiao Tong University School of Medicine Affiliated Ruijin Hospital. His research interests focus on nano-repair medicine.

these methods:  $\text{NOBF}_4$  is unstable at room temperature; PO-PEG is not a commercial product and the process of ligand exchange requires high temperature; and the Lemieux-von Rudloff reagent is not suitable for ligands without a carbon-carbon double bond (such as OctAm) and the high amount of reaction solution is not conducive for the separation of nanomaterials. Hence, it is necessary to develop a new approach that can overcome the limitations of the existing methods.

Dimercaptosuccinic acid (DMSA) contains two sulphhydryl ( $-\text{SH}$ ) groups and two carboxyl ( $-\text{COOH}$ ) groups per molecule, and has been used as a heavy metal antidote in the clinic. According to the hard and soft acids and bases (HSAB) principle,  $-\text{SH}$  is a soft base and  $-\text{COOH}$  is a hard base.<sup>21,22</sup> As decreased radius leads to increased base strength, the  $-\text{COOH}$  in DMSA is a stronger base than OctAm, OA and OAm, which means that DMSA can replace these long-chain ligands. Moreover, with the assistance of  $-\text{SH}$  (soft base) and  $-\text{COOH}$  (hard base), DMSA can simultaneously coordinate soft acids (such as elemental Ag, Au, Pt), hard acids (such as  $\text{Re}^{3+}$ ,  $\text{Ti}^{4+}$ ) and borderline acids (such as  $\text{Cu}^{2+}$ ,  $\text{Zn}^{2+}$ ). Herein, we report a generally applicable method involving using DMSA to endow hydrophobic nanoparticles with water dispersion abilities. As shown in Fig. 1a, a tetrahydrofuran (THF) solution of DMSA was mixed with a cyclohexane solution of hydrophobic nanoparticles. After 48 hours, the nanoparticles were modified with DMSA. This method showed several advantages: firstly, the ability of DMSA to strongly coordinate with most metal elements, and the ability of many inorganic nanomaterials produced using pyrolysis to be modified by DMSA; secondly, the process of ligand exchange being carried out at room temperature, with the nanomaterials being easily separated by carrying out distillation at reduced pressure and subsequent methanol/ethanol rinsing; thirdly, both DMSA and THF being low-cost commercial products; and finally, the surface of DMSA-modified nanomaterials containing abundant  $-\text{SH}$  and  $-\text{COOH}$  groups, a benefit to the further grafting. We believe that our

study will increase the chances for applications of nanomaterials to be made and will provide a method with increased convenience for researchers.

## Results and discussion

Four representative kinds of hydrophobic nanoparticles, namely Ag,  $\text{NaGdF}_4$ ,  $\text{TiO}_2$ , and ZnS, were applied for verifying the performance of this DMSA-based modification method. The procedure used to synthesize these nanomaterials is shown in Fig. 1b. For the synthesis of Ag-OctAm, we poured  $\text{AgNO}_3$  powder directly into a solution of OctAm at  $180^\circ\text{C}$ , and Ag-OctAm nanoparticles were obtained after 0.5 h.<sup>10</sup> For the synthesis of  $\text{NaGdF}_4\text{-OA}$ , first  $\text{GdCl}_3$ , OA and octadecene (ODE) were mixed at  $140^\circ\text{C}$  to obtain Gd precursor, and then this Gd precursor was reacted with sodium fluoride (NaF) powder at  $290^\circ\text{C}$  to obtain  $\text{NaGdF}_4\text{-OA}$ . For the synthesis of  $\text{TiO}_2\text{-OA}$ , we mixed and reacted tetrabutyl titanate ( $\text{Ti}(\text{OC}_4\text{H}_9)_4$ ), OAm, OA, water and ethanol at  $180^\circ\text{C}$  for 18 h to obtain  $\text{TiO}_2\text{-OA}$ .<sup>11,23</sup> For the synthesis of ZnS-OAm, first  $\text{ZnCl}_2$ , trioctylphosphine oxide (TOPO) and OAm were mixed at  $180^\circ\text{C}$  to obtain Zn precursor, and then this Zn precursor was reacted with sulfur solution in OAm at  $320^\circ\text{C}$  to obtain ZnS-OAm.<sup>5</sup> More experimental details can be found in the Methods section.

To clarify the performance of the DMSA-based method, we carried out a series of characterizations of the hydrophobic nanoparticles and DMSA-modified nanoparticles. A photograph of hydrophobic nanoparticles in cyclohexane is shown in Fig. S1a (ESI<sup>†</sup>) and that of DMSA-modified nanomaterials in water is presented in Fig. S1b (ESI<sup>†</sup>). All the solutions were clear and transparent liquids. Then, transmission electron microscopy (TEM) was carried out. Both the Ag-OctAm and Ag-DMSA particles were observed to be spheres with dimensions of  $\sim 8$  nm (Fig. 2a and e), and both the  $\text{NaGdF}_4\text{-OA}$  and  $\text{NaGdF}_4\text{-DMSA}$  particles were observed to be spheres with



Fig. 1 Illustrations of (a) the DMSA-based modification procedure and (b) the procedures used to synthesize Ag-OctAm,  $\text{NaGdF}_4\text{-OA}$ ,  $\text{TiO}_2\text{-OA}$  and ZnS-OAm.



Fig. 2 TEM images of (a) Ag-OctAm, (b) NaGdF<sub>4</sub>-OA, (c) TiO<sub>2</sub>-OA, (d) ZnS-OAm, (e) Ag-DMSA, (f) NaGdF<sub>4</sub>-DMSA, (g) TiO<sub>2</sub>-DMSA and (h) ZnS-DMSA.

dimensions of  $\sim 5$  nm (Fig. 2b and f). In contrast, TiO<sub>2</sub>-OA and TiO<sub>2</sub>-DMSA both formed spindles with dimensions of  $\sim 15$  nm (Fig. 2e and g). And both the ZnS-OAm and ZnS-DMSA particles were observed to be spheres with dimensions of  $\sim 5$  nm (Fig. 2d and h). Hydrodynamic radii were also measured using dynamic light scattering (DLS). The hydrodynamic radii of Ag-OctAm (Fig. S2a, ESI<sup>†</sup>), NaGdF<sub>4</sub>-OA (Fig. S2b, ESI<sup>†</sup>), TiO<sub>2</sub>-OA (Fig. S2c, ESI<sup>†</sup>) and ZnS-OAm (Fig. S2d, ESI<sup>†</sup>) particles

were measured to be 9.09 nm, 6.83 nm, 19.87 nm and 6.43 nm, respectively, in accordance with the TEM image data. X-ray diffraction (XRD) patterns showed the crystal structures of Ag-OctAm (Fig. 3a), NaGdF<sub>4</sub>-OA (Fig. 3b), TiO<sub>2</sub>-OA (Fig. 3c), ZnS-OAm (Fig. 3d), Ag-DMSA (Fig. 3e), NaGdF<sub>4</sub>-DMSA (Fig. 3f), TiO<sub>2</sub>-DMSA (Fig. 3g) and ZnS-DMSA (Fig. 3h) to be in accordance with standard samples, with only a few differences between the XRD patterns of the hydrophobic nanoparticles and those of



Fig. 3 XRD patterns of (a) Ag-OctAm, (b) NaGdF<sub>4</sub>-OA, (c) TiO<sub>2</sub>-OA, (d) ZnS-OAm, (e) Ag-DMSA, (f) NaGdF<sub>4</sub>-DMSA, (g) TiO<sub>2</sub>-DMSA and (h) ZnS-DMSA.

the DMSA-modified nanoparticles. Hence, neither the morphology nor the crystal structure of any of the nanoparticles changed upon the modification being performed.

Fourier-transform infrared spectroscopy (FTIR) data were collected and showed differences between the hydrophobic nanoparticles and the DMSA-modified nanoparticles. As shown in Fig. 4a–d, the four kinds of hydrophobic nanoparticles all showed strong absorption for methylene asymmetric carbon-hydrogen bond (C–H) stretching and methylene symmetric C–H stretching, attributed to the presence of many methylene C–H groups, specifically 28, 30 and 34 of them, per OA molecule, OAm molecule and OctAm molecule, respectively.<sup>24</sup> After ligand exchange, the methylene C–H absorption almost disappeared (Fig. 4e–h), attributed to the DMSA molecule having no methylene C–H. Ultraviolet-visible (UV-Vis) spectra of all related nanomaterials were also acquired (Fig. S3a–S3h, ESI<sup>†</sup>). The differences observed may have been due to the coordination between DMSA and the metal ions.

After the DMSA modification, we measured the hydrodynamic radii of the nanoparticles each at different pH values. The abundant –COOH groups on the surfaces of nanoparticles were expected to dissociate into H<sup>+</sup> and –COO<sup>–</sup> reversibly in aqueous solutions. Generally, higher surface charges enhance electrostatic repulsion between nanoparticles. Hence, a higher pH in the solution was expected to promote the dissociation of –COOH and improve surface charge density, leading to better dispersity of DMSA-modified nanoparticles. As shown in Fig. 5a–d, the particles were determined to be smaller at pH 7.4 than at pH 5.0. Additionally, the absolute value of the zeta potential at pH 7.4 was much greater than that under pH 5.0 (Fig. 5e–h). We also characterized the stability levels of the modified nanomaterials at pH 7.4. As shown in Fig. S4a–S4d (ESI<sup>†</sup>), no significant difference in hydrodynamic size was

observed for Ag-DMSA, NaGdF<sub>4</sub>-DMSA, TiO<sub>2</sub>-DMSA, and ZnS-DMSA between 1-, 7- and 14-day periods. Hence, the modified nanomaterials could remain stable at pH 7.4. In addition, we measured the leakage of Zn<sup>2+</sup> from the ZnS-DMSA surface at pH 5.0. As shown in Fig. S5 (ESI<sup>†</sup>), only 2% of the Zn<sup>2+</sup> was released in 6 days, indicating the stability of ZnS-DMSA in an acid microenvironment. These data confirmed our analysis about the dissociation of –COOH and concurrently indicated that the modification with DMSA occurred.

Finally, we verified that there could be biological applications of DMSA-modified nanoparticles. Due to DMSA bringing –SH and –COOH groups to the surfaces of the nanoparticles, further grafting was expected to be feasible. The aminated polyethylene glycol 2000 (PEG2000-NH<sub>2</sub>) was selected to be reacted with ZnS-DMSA using an amide reaction. C–O–C stretching was not present in the FTIR spectrum of ZnS-DMSA, but appeared in the spectrum of ZnS-PEG (Fig. 6a), indicating the successful modification of PEG.<sup>24</sup> Aminated fluorescein isothiocyanate-polyethylene glycol 2000 (FITC-PEG2000-NH<sub>2</sub>) was also selected for further modification of TiO<sub>2</sub>-DMSA.<sup>25,26</sup> The obtained TiO<sub>2</sub>-FITC was applied for the fluorescence imaging of cytophagy. As shown in Fig. 6b, after 4 hours of co-culture, MG63 cells (human osteosarcoma cells) and PANC-1 cells (human pancreatic cancer cells) both showed the green fluorescence of TiO<sub>2</sub>-FITC as measured using a confocal laser scanning microscope (CLSM). In addition, NaGdF<sub>4</sub>-DMSA was applied for magnetic resonance imaging (MRI). As shown in Fig. 6c, the relaxation rate of NaGdF<sub>4</sub>-DMSA was 6.51 mM<sup>–1</sup> s<sup>–1</sup> at 3.0 T, higher than those of commercial MRI contrast agents such as Magnevist (4.1 mM<sup>–1</sup> s<sup>–1</sup>) and Omniscan (3.3 mM<sup>–1</sup> s<sup>–1</sup>).<sup>27</sup> Finally, the Ag-DMSA was applied for treating cancer due to the widely reported anticancer activity of Ag nanoparticles.<sup>28–30</sup> As shown in Fig. 6d, Ag-DMSA

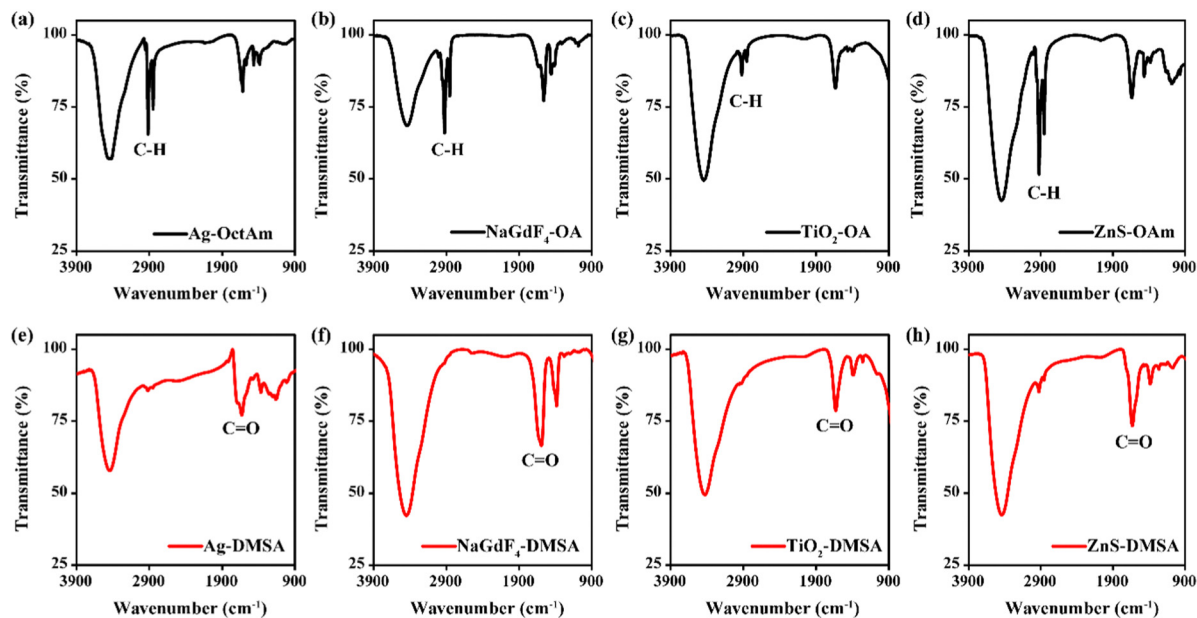


Fig. 4 FTIR spectra of (a) Ag-OctAm, (b) NaGdF<sub>4</sub>-OA, (c) TiO<sub>2</sub>-OA, (d) ZnS-OAm, (e) Ag-DMSA, (f) NaGdF<sub>4</sub>-DMSA, (g) TiO<sub>2</sub>-DMSA and (h) ZnS-DMSA.



Fig. 5 (a)–(d) Hydrodynamic radius values of (a) Ag-DMSA, (b) NaGdF<sub>4</sub>-DMSA, (c) TiO<sub>2</sub>-DMSA and (d) ZnS-DMSA each under two different pH conditions. (e)–(h) Zeta potentials of (e) Ag-DMSA, (f) NaGdF<sub>4</sub>-DMSA, (g) TiO<sub>2</sub>-DMSA and (h) ZnS-DMSA each under two different pH conditions.

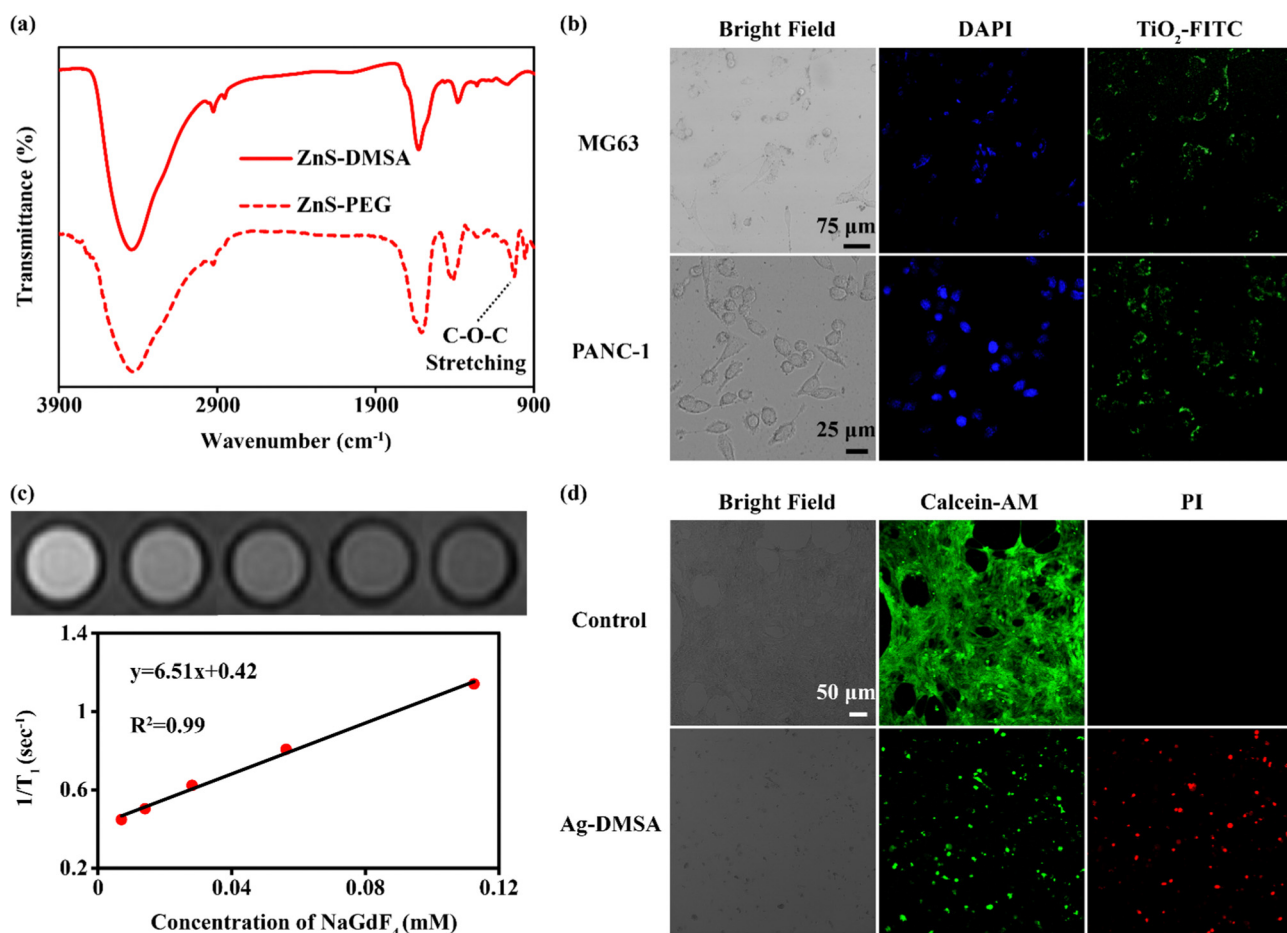


Fig. 6 Further applications of DMSA-modified nanomaterials. (a) FTIR spectrum of ZnS-PEG. (b) CLSM images showing the cytophagy of TiO<sub>2</sub>-FITC. (c) Plot showing the MRI performance of NaGdF<sub>4</sub>-DMSA. (d) Images with calcein-AM and PI stainings showing the anticancer effect of Ag-DMSA.

(20 ppm) can effectively kill 4T1 cells (mouse breast cancer cells) as measured using calcein-AM and propidium iodide (PI) stainings. We also used human umbilicus vein endothelial cells (HUVECs) and 4T1 cells to test the cytotoxicity of Ag-DMSA. As

shown in Fig. S6 (ESI<sup>†</sup>), Ag-DMSA exhibited little toxicity to HUVECs, but were obviously lethal for 4T1 cells. Hence, according to these results, Ag-DMSA showed favorable biocompatibility with normal cells and obvious toxicity to cancer cells, in

accordance with previous research.<sup>31,32</sup> In a word, the DMSA-based modification can widen the applications of hydrophobic nanoparticles.

## Conclusions

In summary, we have developed a generally applicable and easy method for endowing hydrophobic nanoparticles with water dispersion abilities. By mixing a THF solution of DMSA with a cyclohexane solution of hydrophobic nanoparticles, the long-chain ligands are replaced with DMSA, due to the strong coordination abilities of –SH and –COOH groups. In principle, this method can be applied at a large scale. DMSA modification widens the applications of hydrophobic nanoparticles to include MRI and cancer treatment. Additionally, further grafting based on –SH and –COOH groups can be achieved. We hope this method will increase the chances for investigating the applications of nanomaterials.

## Author contributions

Wang H., Lu M., Deng L. and Ni D. conceived the project. Wang H., Fu Z., Ji X., Liu Z. and Yin B. performed the experiments and analyzed the results. Wang H. and Ni D. wrote the manuscript. All the authors discussed the results and commented on the manuscript.

## Conflicts of interest

There are no conflicts to declare.

## Acknowledgements

This research was supported by National Natural Science Foundation of China (82102190), the Foundation of National Facility for Translational Medicine (Shanghai) (TMSK-2021-122), China Postdoctoral Science Foundation (Grant No. 2020M681326), Shanghai Municipal Science and Technology Major Project (No. 2018SHZDZX01) and ZJ Lab, Shanghai Center for Brain-Inspired Technology.

## Notes and references

- D. L. Ni, J. W. Zhang, W. B. Bu, H. Y. Xing, F. Han, Q. F. Xiao, Z. W. Yao, F. Chen, Q. J. He, J. N. Liu, S. J. Zhang, W. P. Fan, L. P. Zhou, W. J. Peng and J. L. Shi, *ACS Nano*, 2014, **8**, 1231–1242.
- H. Wang, B. Lv, Z. M. Tang, M. Zhang, W. Q. Ge, Y. Y. Liu, X. H. He, K. L. Zhao, X. P. Zheng, M. Y. He and W. B. Bu, *Nano Lett.*, 2018, **18**, 5768–5774.
- Y. L. Hou, H. Kondoh, T. Kogure and T. Ohta, *Chem. Mater.*, 2004, **16**, 5149–5152.
- Y. Chong, X. Dai, G. Fang, R. Wu, L. Zhao, X. Ma, X. Tian, S. Lee, C. Zhang, C. Chen, Z. Chai, C. Ge and R. Zhou, *Nat. Commun.*, 2018, **9**, 4861.
- J. Joo, H. B. Na, T. Yu, J. H. Yu, Y. W. Kim, F. Wu, J. Z. Zhang and T. Hyeon, *J. Am. Chem. Soc.*, 2003, **125**, 11100–11105.
- Y. Liu, D. Yao, L. Shen, H. Zhang, X. Zhang and B. Yang, *J. Am. Chem. Soc.*, 2012, **134**, 7207–7210.
- H. Liang, X. Wu, G. Zhao, K. Feng, K. Ni and X. Sun, *J. Am. Chem. Soc.*, 2021, **143**, 15812–15823.
- Y. Lu, Y. J. Xu, G. B. Zhang, D. Ling, M. Q. Wang, Y. Zhou, Y. D. Wu, T. Wu, M. J. Hackett, B. Hyo Kim, H. Chang, J. Kim, X. T. Hu, L. Dong, N. Lee, F. Li, J. C. He, L. Zhang, H. Q. Wen, B. Yang, S. Hong Choi, T. Hyeon and D. H. Zou, *Nat. Biomed. Engine.*, 2017, **1**, 637–643.
- D. Wang, Z. Wang, P. Zhao, W. Zheng, Q. Peng, L. Liu, X. Chen and Y. Li, *Chem. – Asian J.*, 2010, **5**, 925–931.
- D. Wang, T. Xie, Q. Peng and Y. Li, *J. Am. Chem. Soc.*, 2008, **130**, 4016–4022.
- C. T. Dinh, T. D. Nguyen, F. Kleitz and T. O. Do, *ACS Nano*, 2009, **3**, 3737–3743.
- X. Wang, J. Zhuang, Q. Peng and Y. Li, *Nature*, 2005, **437**, 121–124.
- A. Nag, M. V. Kovalenko, J. S. Lee, W. Liu, B. Spokoyny and D. V. Talapin, *J. Am. Chem. Soc.*, 2011, **133**, 10612–10620.
- A. Dong, X. Ye, J. Chen, Y. Kang, T. Gordon, J. M. Kikkawa and C. B. Murray, *J. Am. Chem. Soc.*, 2011, **133**, 998–1006.
- H. B. Na, I. S. Lee, H. Seo, Y. I. Park, J. H. Lee, S. W. Kim and T. Hyeon, *Chem. Commun.*, 2007, 5167–5169.
- Z. G. Chen, H. L. Chen, H. Hu, M. X. Yu, F. Y. Li, Q. Zhang, Z. G. Zhou, T. Yi and C. H. Huang, *J. Am. Chem. Soc.*, 2008, **130**, 3023–3029.
- V. Muhr, S. Wilhelm, T. Hirsch and O. S. Wolfbeis, *Acc. Chem. Res.*, 2014, **47**, 3481–3493.
- G. Tang, J. He, J. Liu, X. Yan and K. Fan, *Exploration*, 2021, **1**, 75–89.
- Y. Zhao, Z. Zhang, Z. Pan and Y. Liu, *Exploration*, 2021, **1**, 20210089.
- J. Ouyang, A. Xie, J. Zhou, R. Liu, L. Wang, H. Liu, N. Kong and W. Tao, *Chem. Soc. Rev.*, 2022, **51**, 4996–5041.
- R. G. Pearson, *J. Chem. Educ.*, 1968, **45**, 581–587.
- R. G. Pearson, *J. Chem. Educ.*, 1968, **45**, 643–648.
- W. W. Su, H. Wang, T. Wang, X. Li, Z. M. Tang, S. Zhao, M. Zhang, D. N. Li, X. W. Jiang, T. Gong, W. Yang, C. J. Zuo, Y. L. Wu and W. B. Bu, *Adv. Sci.*, 2020, **7**, 8.
- B. H. Stuart, *Infrared Spectroscopy: Fundamentals and Applications*, 2004.
- X. Huang, C. Liu, N. Kong, Y. Xiao, A. Yurdagul, Jr., I. Tabas and W. Tao, *Nat. Protoc.*, 2022, **17**, 748–780.
- N. Kong, R. Zhang, G. Wu, X. Sui, J. Wang, N. Y. Kim, S. Blake, D. De, T. Xie, Y. Cao and W. Tao, *Proc. Natl. Acad. Sci. U. S. A.*, 2022, **119**, e2112696119.
- Z. Liu, M. Zhao, H. Wang, Z. Fu, H. Gao, W. Peng, D. Ni, W. Tang and Y. Gu, *J. Nanobiotechnol.*, 2022, **20**, 170.
- V. Porto, E. Borrajo, D. Buceta, C. Carneiro, S. Huseyinova, B. Dominguez, K. J. E. Borgman, M. Lakadamyali, M. F. Garcia-Parajo, J. Neissa, T. Garcia-Caballero, G. Barone, M. C. Blanco, N. Busto, B. Garcia, J. M. Leal, J. Blanco, J. Rivas, M. A. Lopez-Quintela and F. Dominguez, *Adv. Mater.*, 2018, e1801317.

- 29 R. Foldbjerg, D. A. Dang and H. Autrup, *Arch. Toxicol.*, 2011, **85**, 743–750.
- 30 X. F. Zhang, Z. G. Liu, W. Shen and S. Gurunathan, *Int. J. Mol. Sci.*, 2016, **17**, 1534.
- 31 D. Trachootham, J. Alexandre and P. Huang, *Nat. Rev. Drug Discovery*, 2009, **8**, 579–591.
- 32 P. V. AshaRani, G. Low Kah Mun, M. P. Hande and S. Valiyaveetil, *ACS Nano*, 2009, **3**, 279–290.